How to cite: Angew. Chem. Int. Ed. 2023, e202314595
doi.org/10.1002/anie.202314595

VIP Bioimaging Very Important Paper

Exchangeable Self-Assembled Lanthanide Antennas for PLIM Microscopy

Alvaro Ruiz-Arias, Francisco Fueyo-González, Carolina Izquierdo-García, Amparo Navarro, Marta Gutiérrez-Rodríguez, Rosario Herranz, Chiara Burgio, Antonio Reinoso, Juan M. Cuerva, Angel Orte, and Juan A. González-Vera**

Abstract: Lanthanides have unique photoluminescence (PL) emission properties, including very long PL lifetimes. This makes them ideal for biological imaging applications, especially using PL lifetime imaging microscopy (PLIM). PLIM is an inherently multidimensional technique with exceptional advantages for quantitative biological imaging. Unfortunately, due to the required prolonged acquisitions times, photobleaching of lanthanide PL emission currently constitutes one of the main drawbacks of PLIM. In this study, we report a small aqueous-soluble, lanthanide antenna, 8-methoxy-2-oxo-1,2,4,5-tetrahydrocyclopenta[*de*]quinoline-3-phosphonic acid, **PAnt**, specifically designed to dynamically interact with lanthanide ions, serving as exchangeable dye aimed at mitigating photobleaching in PLIM microscopy *in cellulo*. Thus, self-assembled lanthanide complexes that may be photobleached during image acquisition are continuously replenished by intact lanthanide antennas from a large reservoir. Remarkably, our self-assembled lanthanide complex clearly demonstrated a significant reduction of PL photobleaching when compared to well-established lanthanide cryptates, used for bioimaging. This concept of exchangeable lanthanide antennas opens new possibilities for quantitative PLIM bioimaging.

Thanks to the unique photoluminescence (PL) emission properties of lanthanide cations (Ln^{3+}), lanthanide-based probes have emerged as powerful chemical tools for cellular imaging, ushering in a revolution in the field of chemical biology. Among these characteristics, they emit very narrow line-like peaks specific of each ion, and present exceptionally long PL lifetimes, τ_{PL}, on the order of hundreds of microseconds to milliseconds, in stark contrast to conventional organic dyes.[1] These features were early exploited to design homogeneous time-resolved fluoroimmunoassays with high sensitivity,[2] such as dissociation-enhanced lanthanide fluorescence immunoassay (DELFIA)[3] or the lanthanide chelate excite (LANCE) assays.[4] In addition, the emission of lanthanide ions also allows exciting biological imaging applications.[5] A key aspect in using lanthanide PL emission in biological imaging applications is the requirement of an indirect excitation method involving photo-excited energy transfer using suitable organic chromophores, known as antennas.[6] One of the most straightforward and effective approaches to achieve this effect involve the formation of soluble lanthanide complexes and cryptates, where the antenna can directly participate. Currently, there is a critical demand of new antennas and complexes capable of directly assembling in water to sensitize lanthanide PL.

Among the specialized techniques for biological imaging using lanthanide emission, PL lifetime imaging microscopy

[*] A. Ruiz-Arias, Prof. A. Orte, Dr. J. A. González-Vera
Nanoscopy-UGR Laboratory. Departamento de Fisicoquímica, Unidad de Excelencia de Química Aplicada a Biomedicina y Medioambiente, Facultad de Farmacia, Universidad de Granada
Campus Cartuja, 18071 Granada (Spain)
E-mail: angelort@ugr.es
gonzalezvera@ugr.es

Dr. F. Fueyo-González, C. Izquierdo-García,
Dr. M. Gutiérrez-Rodríguez, Prof. R. Herranz, Dr. J. A. González-Vera
Instituto de Química Médica (IQM-CSIC)
Juan de la Cierva 3, 28006 Madrid (Spain)

Dr. A. Navarro
Departamento de Química Física y Analítica, Facultad de Ciencias Experimentales, Universidad de Jaén
23071 Jaén (Spain)

Dr. M. Gutiérrez-Rodríguez
PTI-Global Health CSIC
Juan de la Cierva 3, 28006 Madrid (Spain)

Dr. C. Burgio, A. Reinoso
Departamento de Bioquímica y Biología Molecular II, Facultad de Farmacia, Universidad de Granada
Campus Cartuja, 18071 Granada (Spain)

Prof. J. M. Cuerva
Departamento de Química Orgánica, Unidad de Excelencia de Química Aplicada a Biomedicina y Medioambiente, Facultad de Ciencias, Universidad de Granada
Campus Fuentenueva, 18071 Granada (Spain)

Dr. F. Fueyo-González
Current address: Department of Medicine, Translational Transplant Research Center, Immunology Institute, Icahn School of Medicine at Mount Sinai
New York (USA)

(PLIM) stands out. PLIM is an inherently multidimensional technique that comprises both the PL intensity (total number of photons) and the PL lifetime information,[7] allowing performing time-gated filtering of the images for an efficient removal of any contributions of interfering species and autofluorescence for a quantitative detection of low concentrations of the luminophores.[2b] PLIM is a potent methodology for quantitative imaging, specially due to the independency of the PL lifetime with the luminophore concentration and the laser excitation power.[8] Unfortunately, photobleaching of lanthanide PL emission currently constitutes one of the main drawbacks and challenges in PLIM microscopy, especially due to the prolonged acquisitions times required to obtain with high fidelity the highest spatial resolution in live-cell experiments. Attempts to minimize photobleaching include the development of novel photostable lanthanide complexes and cryptates[9] and other hybrid materials[10] that contribute to signal-to-noise ratio and thus resolution.

An alternative and elegant way to bypass photobleaching in imaging, used in PAINT (Point Accumulation for Imaging in Nanoscale Topography) and super-resolution microscopy, involve the use of exchangeable dyes.[11] This involves using a pool of dyes that transiently bind to the desired target in situ and dynamically interchange, so that photobleached dyes are replaced by fresh molecules, extending acquisition times and improving photon statistics and spatial resolution. We decided to extrapolate this concept to PLIM lanthanide imaging by using antennas forming transient, dynamic luminescent complexes *in cellulo*. Therefore, self-assembled lanthanide complexes that may be photobleached during image acquisition are continuously replenished by intact lanthanide antennas from a large reservoir (Figure 1). This approach requires rapid interchange rates of the antennas with the lanthanide ions, as well as lanthanide complexes thermodynamically stable and capable of directly assembling in aqueous media *in cellulo*, thereby making their application in biological systems possible. However, most of self-assembling lanthanide complexes show PL deactivation in the presence of water due to the interactions between the surrounding aqueous environment and the antenna-lanthanide complex.[6b,12] As a result, very few examples of lanthanide antennas that self-assemble in water have been described in the literature[12a][13] In this sense, we recently described a lanthanide antenna (8-methoxy-2-oxo-1,2- dihydrocyclopenta[*de*]quinoline-3-carboxylic acid), able to directly coordinate Tb(III) and Eu(III), sensitizing their emission in water, and useful as a luminescent sensor of biothiols for the study of human cells of the immune system by flow cytometry.[14]

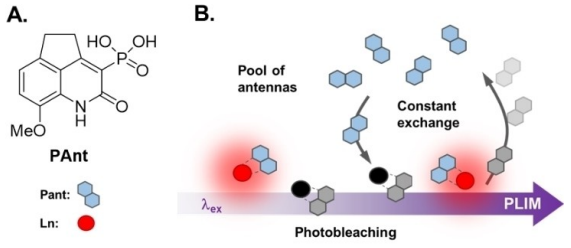

Figure 1. A) Chemical structure of exchangeable lanthanide antenna **PAnt**. B) Illustration of the principle of exchangeable self-assembled lanthanide (Ln) antenna **PAnt** to bypass photobleaching in PLIM microscopy *in cellulo*.

In this work, we focus on developing enhanced aqueous-soluble, self-assembled, lanthanide antennas specifically designed to serve as exchangeable dyes aimed at mitigating photobleaching in PLIM microscopy *in cellulo*. Hence, we have developed a novel modified luminophore containing a phosphonic acid moiety (8-methoxy-2-oxo-1,2,4,5-tetrahydrocyclopenta[*de*]quinoline-3-phosphonic acid, Figure 1). This Phosphonic acid Antenna (**PAnt**) was synthesized from its diethyl phosphonate[12c] by treatment with trimethylsilyl bromide in CH_3CN (full details are shown in the Supporting Information, SI). The presence of the phosphonic acid group provides increased affinity for lanthanide ions compared to its carboxylic acid counterpart.

In water **PAnt** exhibited two absorption maxima at 310 and 345 nm in the UV region of the visible spectrum (Figure S2). In contrast, a single fluorescence emission band was detected, independent of the excitation wavelength, confirming the direct emission from the first excited singlet state (Figure S2). The quantum yield obtained in water (using $\lambda_{ex} = 320$ and 350 nm, see Supporting Information for details) was of 0.14, which was in the same range as those reported for other quinolin-2(1*H*)-ones.[12c]

For **PAnt** to be an effective lanthanide antenna in aqueous solution, sufficiently stable, self-assembled complexes should be formed; this formation would provide the optimal conditions for subsequent energy transfer and sensitization. Thus, we first performed a screening to examine the capability of **PAnt** to directly bind lanthanide ions in aqueous solution (54 μM) sensitizing their luminescence. Notably, upon the addition of 1 and 2 equivalents of $TbCl_3$, $EuCl_3$, $DyCl_3$ or $SmCl_3$, lanthanide PL emission was exhibited for Tb(III) and Eu(III) (Figure S3). Then we carried out a titration of a solution of **PAnt** (27 μM) in H_2O with increasing concentrations of $TbCl_3$ or $EuCl_3$ (Figure 2). The formation of an effective self-assembled complex between **PAnt** and the corresponding lanthanide ion (Tb(III) or Eu(III)) was evidenced by the appearance of significant bands of the sensitized luminescence of each lanthanide cation, mainly the $^5D_4 \rightarrow {}^7F_6$ (490 nm) and $^5D_4 \rightarrow {}^7F_5$ (540 – 550 nm) Tb(III) bands and the $^5D_0 \rightarrow {}^7F_2$ Eu(III) band at 615 nm, and by the quenching of the antenna emission at 445 nm due to energy transfer (98.6 ± 0.3 % or 99.6 ± 0.1 % quenching efficiency with 2 equivalents of Tb(III) or Eu(III) added, respectively) (Figures 2A–B). Moreover, the effective energy transfer was confirmed employing phosphorescence spectroscopy in the titrations; thus, the emission of the antenna was eliminated by applying a delayed detection time gate, leaving only the typical sensitized emissions of the lanthanide ions (Figures 2C–D). The PL lifetime τ_{PL} values of the complexes of **PAnt** with Tb(III) and Eu(III) were 0.117 ± 0.003 ms and 0.307 ± 0.007 ms, respectively.

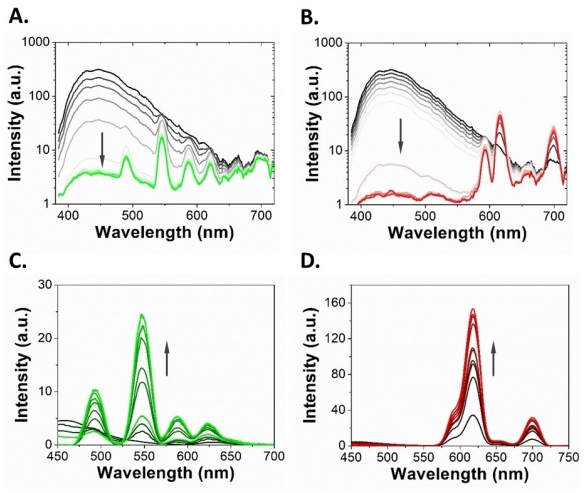

Figure 2. Emission PL spectra (λ_{ex} = 320 nm) of the titrations of **PAnt** (27 μM) with increasing concentrations of A) Tb(III) or B) Eu(III) (from 0 to 86.2 μM). Time-gated phosphorescence spectra (λ_{ex} = 320 nm) of the titrations of **PAnt** (27 μM) with increasing concentrations of C) Tb(III) or D) Eu(III) (from 0 to 86.2 μM). Arrows indicate increasing concentrations of Tb(III) or Eu(III).

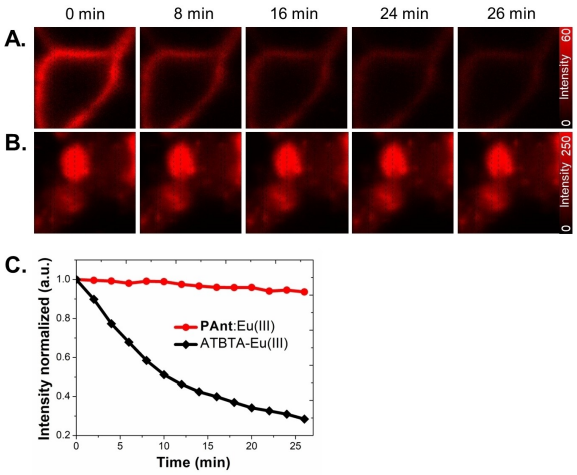

Figure 3. A–B) PLIM images of HEK-293 cells with **PAnt**:Eu(III) (15 : 30 μM, A) or the non-exchangeable cryptate ATBTA-Eu(III) (1 μM, B). Cells were imaged continuously at 375 nm for 26 min. C) Comparison of the Eu(III) PL signal versus time.

The complexes formed with ligand **PAnt** were thermodynamically stable and soluble in water, thus allowing cellular PLIM imaging. Nevertheless, the fact that such complexes are self-assembled, and the antennas are not part of a cryptate, allows the dynamic exchange of the coordination spheres. Thus, we tested our exchangeable lanthanide antenna **PAnt** for its applicability in PLIM microscopy in living cells and compared its photostability to that of the non-exchangeable lanthanide cryptate ATBTA–Eu(III). Initially, we explored whether a constant and dynamic exchange of antenna **PAnt** and Eu(III) occurs *in cellulo*, which should enable multiple rounds of PLIM imaging on the same cell without a significant loss of PL signal. Optimal concentrations of antenna **PAnt** (ranging from 15–30 μM) and Eu(III) (ranging from 30–60 μM) were required in the imaging buffer to ensure a constant, dynamic formation of the corresponding complex **PAnt**:Eu(III) in living cells. Using 2 equivalents of the lanthanide ion respect to the antenna fostered 1 : 1 stoichiometric interactions due to entropic arguments, as well as maximum **PAnt**→Eu(III) energy transfer. To determine the degree of photobleaching, we added the self-assembled exchangeable lanthanide antenna **PAnt** (15 μM) and Eu(III) (30 μM) or the non-exchangeable cryptate ATBTA–Eu(III) (1 μM) to human embryonic kidney (HEK)-293 cells and then we took a sequence of PLIM images of the complexes inside cells (λ_{ex} = 375 nm, Figure 3 and SI Video). Importantly, quantitative analysis of PLIM PL intensity over time (0 to 26 min) under continuous irradiation displayed an outstanding photostability in the case of the self-assembled exchangeable lanthanide complex **PAnt**:Eu(III), which maintained a consistent PL signal over time. In contrast, PLIM PL intensity of the non-exchangeable cryptate ATBTA–Eu(III) exhibited a significant level of photobleaching, dropping by 72 % within 26 min. Moreover, the large size of the ATBTA–Eu(III) complex hindered its localization inside cells, whereas the smaller size of the **PAnt**:Eu(III) complex made its cellular intake straightforward. This result clearly shows the concept of exchangeable lanthanide self-assembled, complex **PAnt**:Eu(III) remarkably enhancing the photostability for PLIM imaging, paving the way for its application in a variety a biological assays.

Once we had demonstrated the outstanding photostability of our dynamic, self-assembled lanthanide complex **PAnt**:Eu(III) for PL microscopy *in cellulo*, next we examined whether the complexes targeted specific subcellular sites and studied τ_{PL} values using PLIM. For this purpose, we added the antenna **PAnt** (15 μM) and Tb(III) or Eu(III) ions (30 μM) to (HEK)-293 cells and took PLIM images of the complexes (Figure 4). In all the cellular images analyzed, lanthanide PL emission was unequivocally detected within the cytoplasm and the cellular nucleus, as demonstrated by the submillisecond τ_{PL} values (Figure S4), allowing a layer of contrast in the complete visualization of cells. The pseudo-colored PLIM images of **PAnt**:Eu(III) (Figures 4A and S4) and **PAnt**:Tb(III) (Figures 4B and S4) complexes usually exhibited subtle lifetime τ_{PL} differences between the cytoplasm and the nuclear region.[5c] We quantified the average τ_{PL} values of **PAnt**:Eu(III) and **PAnt**:Tb(III) (Figure S5), segmenting the cellular cytoplasm and the nucleus and obtaining 0.46 ± 0.01 ms and 0.50 ± 0.02 ms for **PAnt**:Eu(III), respectively; for **PAnt**:Tb(III), we obtained broader distributions, with average τ_{PL} values of 0.55 ± 0.07 ms and 0.69 ± 0.05 ms for the cytoplasm and nucleus, respectively. Regarding the whole population, across the different images collected, no statistical significance was found between the τ_{PL} values in the nucleus and cytoplasm for the emissive complexes; additionally, eye inspection of the PLIM images (Figures 4A–B, and S4) revealed a correlation of larger lifetime values within the nucleus. This phenomenon occurred due to the more protected environment and better formation of the complexes within the nuclear region.

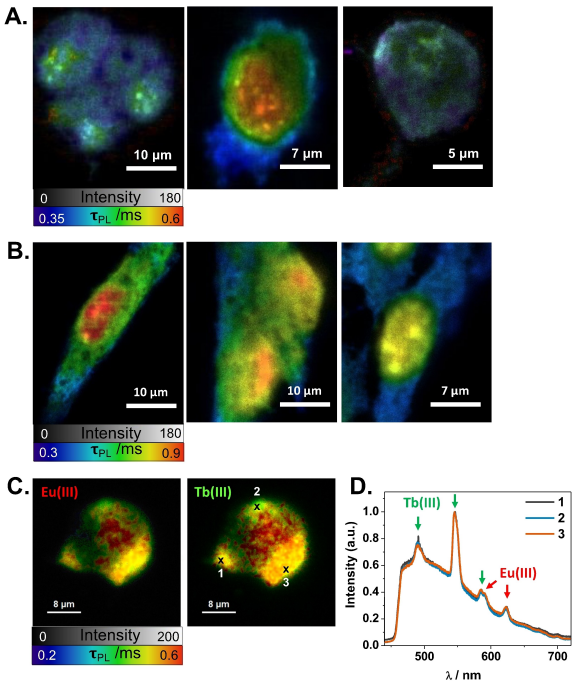

Figure 4. A–B) PLIM images of HEK-293 cells with **PAnt**:Eu(III) (15 : 30 µM, A) or **PAnt**:Tb(III) complexes (15 : 30 µM, B). λ_{ex} = 375 nm (a train of excitation pulses during 200 µs, followed by a 5 ms detection window). The detection was performed using a 580–630 nm bandpass filter for Eu(III) or a 533–558 nm bandpass filter for Tb(III). C) **PAnt**: Eu(III) and **PAnt**:Tb(III) PLIM imaging of live HEK-293 cells incubated with 31 µM **PAnt**, 46 µM Tb(III), and 2.1 µM Eu(III). D) Normalized emission spectra collected by irradiating points 1–3 marked in panel C).

Additionally, note that, especially for the **PAnt**:Tb(III) complex, the τ_{PL} values obtained in cellular media were larger than those directly obtained in aqueous solutions, thus confirming the lower water activity, further protection of the coordination sphere from water molecules, and lower quenching in the highly crowded cellular environment. In any case, the long τ_{PL} values of the complexes were particularly effective in removing cellular autofluorescence (Figure S4).

A particular property of the combination of **PAnt** (blue emission), with Tb(III) (green emission) and Eu(III) (red emission) is that we have the elements in place to design an RGB emitter. By applying a tuned combination of the three elements, we explored the possibility of obtaining white light emission in living cells. This is particularly interesting, since white light emitters in living cells have been proposed as an advanced platform for multicolor and spectral sensing strategies.[15] In addition, white light emitters in liquid phase have many technological applications as lightning sources and emissive inks.[16] First, we optimized the relative concentrations of each component in aqueous solution (Table S1, Figures S6 and S7A–B) and in 1 % agarose gels (Table S1, Figures S6 and S7C–D) to consider the dispersive character of the intracellular media. Then, we used the optimized conditions in gels as a starting point to achieve white light emission within living HEK-293 cells and checked this emission with dual-color PLIM imaging and spectral imaging. Figures 4C and S9–S11 (SI) show simultaneous **PAnt**:Eu(III) and **PAnt**:Tb(III) PLIM imaging of HEK-293 cells incubated with both complexes using 31 µM of **PAnt**, 46 µM of Tb(III), and 2.1 µM of Eu(III). These concentrations followed the same proportions as those obtained for white light emission in gels and showed negligible toxicity in living cells (Figure S12). The average τ_{PL} values (Figure S8) peaked at approximately 0.5 ms, as expected, exhibiting slightly larger values within the nucleus. The lifetime for the Tb(III):**PAnt** complex was slightly lower than those shown in Figure S5 due to the larger concentration of Tb(III); such a high Tb(III) concentration favored substoichiometric complex formation, leading to larger quenching and thus lower average τ_{PL} values. Importantly, our PLIM microscope was equipped with spectral imaging; thus, we collected emission spectra at different points within the cells (Figures 4C–D and S9–S11), clearly demonstrating the simultaneous emission of both complexes in all the cellular regions on top of the autofluorescence background (spectral imaging could not be obtained in PLIM mode, only under continuous illumination). Although a cutoff dichroic mirror was necessary in the microscope, which eliminated emissions below 460 nm, and the contribution of the cellular autofluorescence shifted the emission coordinates in the chromaticity diagram, we demonstrated *quasi*-white light emission from living cells, supporting the versatility of our system. Moreover, the combined use of two different complexes paved the way for color-coding[13] and multiplexed sensing applications[17] *in cellulo*, taking advantage of background-free PLIM imaging.

In the present work, we propose a new method for overcoming the challenges of photobleaching in PLIM microscopy using lanthanide-based luminophores. The method involves using the exchangeable lanthanide antenna **PAnt** capable of self-assembling with trivalent lanthanide ions in water thus sensitizing their luminescence. The antenna molecules in the transient complexes can be dynamically replenished as they photobleach.

The self-assembled complexes of **PAnt** with both Eu(III) and Tb(III) that formed in water paved the way for multiple biological and technological applications. In contrast to other small-molecule lanthanide complexes in organic solvents[18] or in the solid state,[19] our complexes in water provided further biocompatibility, negligible cytotoxicity and their self-assembly behavior resulted in simple preparation protocols. Another advantage of this novel strategy lies in the simplicity of the self-assembly strategy, in contrast to bulky, synthetically demanding cryptates, acknowledging the less efficient emission of the self-assembled complexes due to partial water quenching and the equilibrium-driven distribution of species. Our exchangeable, self-assembled probes represent a completely different concept compared to established designs of lanthanide luminescent agents for cellular imaging.[5a,b,6a,12b] Remarkably, our self-assembled lanthanide complex clearly demonstrated a significant reduction of lanthanide PL photobleaching when compared to ATBTA–Eu(III), a well-established lanthanide cryptate commonly used for bioimaging in living cells.[1b,20] The

proposed method for using exchangeable lanthanide antennas could overcome the limitation for kinetic studies or spatial resolution associated to photobleaching events, thus providing a promising new approach for overcoming the challenges in quantitative PLIM microscopy with lanthanide probes.

Acknowledgements

This work was supported by grant PID2020-114256RB-I00 funded by AEI/10.13039/501100011033; grant PID2019-104366RB-C22 funded by AEI/10.13039/501100011033/FEDER "Una manera de hacer Europa"; grants P21_00212, A-FQM-386-UGR20 and 2021/00627/001-FEDER_UJA_2020 funded by FEDER/Junta de Andalucía-Consejería de Transformación Económica, Industria, Conocimiento y Universidades; CSIC grant 202180E073; and Acción 1 from Universidad de Jaén. Funding for open access charge: Universidad de Granada/CBUA. A.R.-A. thanks the Spanish Ministerio de Educación y Formación Profesional for the FPU Ph.D. scholarship.

Conflict of Interest

The authors declare no conflict of interest.

Data Availability Statement

The data that support the findings of this study are available from the corresponding author upon reasonable request.

Keywords: Bioimaging · Lanthanide Antenna · Luminescence · PLIM · Photostability

[1] a) J.-C. G. Bünzli, S. V. Eliseeva, in *Lanthanide Luminescence: Photophysical, Analytical and Biological Aspects* (Eds.: P. Hänninen, H. Härmä), Springer, Berlin, Heidelberg, **2011**, pp. 1–45; b) U. Cho, J. K. Chen, *Cell Chem. Biol.* **2020**, *27*, 921–936.

[2] a) F. Degorce, A. Card, S. Soh, E. Trinquet, G. P. Knapik, B. Xie, *Curr. Chem. Genomics* **2018**, *3*, 22–32; b) E. Garcia-Fernandez, S. Pernagallo, J. A. González-Vera, M. J. Ruedas-Rama, J. J. Díaz-Mochón, A. Orte, in *Fluorescence in Industry, Vol. 18* (Ed.: B. Pedras), Springer International Publishing, Cham, **2019**, pp. 213–267.

[3] I. Hemmilä, S. Dakubu, V.-M. Mukkala, H. Siitari, T. Lövgren, *Anal. Biochem.* **1984**, *137*, 335–343.

[4] J. Karvinen, P. Hurskainen, S. Gopalakrishnan, D. Burns, U. Warrior, I. Hemmilä, *SLAS Discovery* **2002**, *7*, 223–231.

[5] a) J. C. Bunzli, *Interface Focus* **2013**, *3*, 20130032; b) J. Monteiro, *Molecules* **2020**, *25*, 2089; c) J. Yu, D. Parker, R. Pal, R. A. Poole, M. J. Cann, *J. Am. Chem. Soc.* **2006**, *128*, 2294–2299; d) X. Zhu, X. Wang, H. Zhang, F. Zhang, *Angew. Chem. Int. Ed.* **2022**, *61*, e202209378.

[6] a) G. Muller, *Dalton Trans.* **2009**, 9692–9707; b) M. H. V. Werts, *Sci. Prog.* **2005**, *88*, 101–131.

[7] a) K. Y. Zhang, Q. Yu, H. Wei, S. Liu, Q. Zhao, W. Huang, *Chem. Rev.* **2018**, *118*, 1770–1839; b) P. S. Chelushkin, S. P. Tunik, in *Progress in Photon Science: Recent Advances* (Eds.: K. Yamanouchi, S. Tunik, V. Makarov), Springer International Publishing, Cham, **2019**, pp. 109–128.

[8] a) Q. Wu, K. Y. Zhang, P. Dai, H. Zhu, Y. Wang, L. Song, L. Wang, S. Liu, Q. Zhao, W. Huang, *J. Am. Chem. Soc.* **2020**, *142*, 1057–1064; b) J. Zhou, J. Li, K. Y. Zhang, S. Liu, Q. Zhao, *Coord. Chem. Rev.* **2022**, *453*, 214334.

[9] a) T. Emelina, A. Mirochnik, I. Kalinovskaya, *J. Lumin.* **2021**, *238*, 118274; b) Y. H. Pham, V. A. Trush, A. N. Carneiro Neto, M. Korabik, J. Sokolnicki, M. Weselski, O. L. Malta, V. M. Amirkhanov, P. Gawryszewska, *J. Mater. Chem. C* **2020**, *8*, 9993–10009.

[10] a) M. M. Nolasco, P. M. Vaz, V. T. Freitas, P. P. Lima, P. S. André, R. A. S. Ferreira, P. D. Vaz, P. Ribeiro-Claro, L. D. Carlos, *J. Mater. Chem. A* **2013**, *1*, 7339–7350; b) M. Fernandes, V. de Zea Bermudez, R. A. Sá Ferreira, L. D. Carlos, A. Charas, J. Morgado, M. M. Silva, M. J. Smith, *Chem. Mater.* **2007**, *19*, 3892–3901.

[11] a) M. Glogger, D. Wang, J. Kompa, A. Balakrishnan, J. Hiblot, H. D. Barth, K. Johnsson, M. Heilemann, *ACS Nano* **2022**, *16*, 17991–17997; b) J. Kwon, M. S. Elgawish, S.-H. Shim, *Adv. Sci.* **2022**, *9*, 2101817; c) J. Chen, C. Wang, W. Liu, Q. Qiao, H. Qi, W. Zhou, N. Xu, J. Li, H. Piao, D. Tan, X. Liu, Z. Xu, *Angew. Chem. Int. Ed.* **2021**, *60*, 25104–25113; d) J. Kompa, J. Bruins, M. Glogger, J. Wilhelm, M. S. Frei, M. Tarnawski, E. D'Este, M. Heilemann, J. Hiblot, K. Johnsson, *J. Am. Chem. Soc.* **2023**, *145*, 3075–3083; e) P. Carravilla, A. Dasgupta, G. Zhurgenbayeva, D. I. Danylchuk, A. S. Klymchenko, E. Sezgin, C. Eggeling, *Biophys. Rep.* **2021**, *1*, 100023; f) C. Spahn, J. B. Grimm, L. D. Lavis, M. Lampe, M. Heilemann, *Nano Lett.* **2019**, *19*, 500–505.

[12] a) M. R. George, C. A. Golden, M. C. Grossel, R. J. Curry, *Inorg. Chem.* **2006**, *45*, 1739–1744; b) D. Parker, J. D. Fradgley, K. L. Wong, *Chem. Soc. Rev.* **2021**, *50*, 8193–8213; c) F. Fueyo-González, E. Garcia-Fernandez, D. Martinez, L. Infantes, A. Orte, J. A. González-Vera, R. Herranz, *Chem. Commun.* **2020**, *56*, 5484–5487.

[13] N. Wartenberg, O. Raccurt, E. Bourgeat-Lami, D. Imbert, M. Mazzanti, *Chem. Eur. J.* **2013**, *19*, 3477–3482.

[14] F. Fueyo-González, L. Espinar-Barranco, R. Herranz, I. Alkorta, L. Crovetto, M. Fribourg, J. M. Paredes, A. Orte, J. A. González-Vera, *ACS Sens.* **2022**, *7*, 322–330.

[15] a) J. Wang, W. Lin, W. Li, *Biomaterials* **2013**, *34*, 7429–7436; b) Y.-S. Yang, Z.-H. Yuan, X.-P. Zhang, J.-F. Xu, P.-C. Lv, H.-L. Zhu, *J. Mater. Chem. B* **2019**, *7*, 2911–2914.

[16] S. Santhosh Babu, J. Aimi, H. Ozawa, N. Shirahata, A. Saeki, S. Seki, A. Ajayaghosh, H. Möhwald, T. Nakanishi, *Angew. Chem. Int. Ed.* **2012**, *51*, 3391–3395.

[17] M. S. Tremblay, M. Halim, D. Sames, *J. Am. Chem. Soc.* **2007**, *129*, 7570–7577.

[18] O. Kotova, S. Comby, C. Lincheneau, T. Gunnlaugsson, *Chem. Sci.* **2017**, *8*, 3419–3426.

[19] A. Balamurugan, A. K. Gupta, R. Boomishankar, M. Lakshmipathi Reddy, M. Jayakannan, *ChemPlusChem* **2013**, *78*, 737–745.

[20] a) T. Nishioka, J. Yuan, Y. Yamamoto, K. Sumitomo, Z. Wang, K. Hashino, C. Hosoya, K. Ikawa, G. Wang, K. Matsumoto, *Inorg. Chem.* **2006**, *45*, 4088–4096; b) U. Cho, D. P. Riordan, P. Ciepla, K. S. Kocherlakota, J. K. Chen, P. B. Harbury, *Nat. Chem. Biol.* **2018**, *14*, 15–21.

Manuscript received: September 28, 2023
Accepted manuscript online: November 22, 2023
Version of record online: November 22, 2023

Communications

Bioimaging

A. Ruiz-Arias, F. Fueyo-González, C. Izquierdo-García, A. Navarro, M. Gutiérrez-Rodríguez, R. Herranz, C. Burgio, A. Reinoso, J. M. Cuerva, A. Orte,* J. A. González-Vera* _____ **e202314595**

Exchangeable Self-Assembled Lanthanide Antennas for PLIM Microscopy

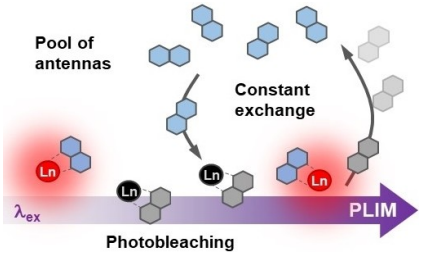

We report a small aqueous-soluble lanthanide antenna (**PAnt**) specifically designed to dynamically interact with lanthanide ions and act as an exchangeable dye, aiming at mitigating photobleaching in PLIM microscopy *in cellulo*. Our self-assembled lanthanide complex exhibited an exceptional photostability compared to traditional lanthanide cryptates, marking a significant advance in quantitative PLIM bioimaging.